Neural Networks ▮ (▮▮▮▮) ▮▮▮–▮▮▮

Contents lists available at ScienceDirect

Neural Networks

journal homepage: www.elsevier.com/locate/neunet

2009 Special Issue

Hippocampus, microcircuits and associative memory

Vassilis Cutsuridis [a,*], Thomas Wennekers [b]

[a] Department of Computing Science and Mathematics, University of Stirling, Stirling, FK9 4LA, UK
[b] Centre for Theoretical and Computational Neuroscience, University of Plymouth, Plymouth, UK

ARTICLE INFO

Article history:
Received 2 February 2009
Received in revised form 20 May 2009
Accepted 14 July 2009

Keywords:
Hippocampus
Microcircuit
Associative memory
Hebb
STDP
Interneurons
Rhythms

ABSTRACT

The hippocampus is one of the most widely studied brain region. One of its functional roles is the storage and recall of declarative memories. Recent hippocampus research has yielded a wealth of data on network architecture, cell types, the anatomy and membrane properties of pyramidal cells and interneurons, and synaptic plasticity. Understanding the functional roles of different families of hippocampal neurons in information processing, synaptic plasticity and network oscillations poses a great challenge but also promises deep insight into one of the major brain systems. Computational and mathematical models play an instrumental role in exploring such functions. In this paper, we provide an overview of abstract and biophysical models of associative memory with particular emphasis on the operations performed by the diverse (inter)neurons in encoding and retrieval of memories in the hippocampus.

1. Introduction

1.1. Associative memory

Associative memory is one of the oldest artificial neural network (ANN) paradigms. The concept of the associative memory was first introduced by the formalism of a correlation matrix (Kohonen, 1978; Palm, 1982, 1980; Steinbuch, 1961; Willshaw, Buneman, & Longuet-Higgins, 1969). In the correlation matrix, memory patterns were encoded as the activity patterns across a network of computing units. Patterns were stored in memory by Hebbian modification of the connections between the computing units. A memory was recalled when an activity pattern that was a partial or noisy version of a stored pattern was instantiated in the network. Network activity then evolved to the complete stored pattern as appropriate units were recruited to the activity pattern, and noisy units were removed, by threshold-setting of unit activity. Memory capacity for accurate recall was strongly dependent on the form of patterns to be stored and the learning rule employed (Palm & Sommer, 1996).

An example of an associative memory comprising of 6 input channels interacting with 6 output channels forming a matrix of 36 elements is depicted in Fig. 1. Activity in a channel is represented by 1, and inactivity by 0. Associations between the input and output patterns $(x^i, y^i), i = 1, 2, \ldots$, are formed via a Hebbian learning rule, where co-activation of the input and output units results in an irreversible transition of synapses from 0 to 1. Such associations between binary stimulus events are then stored in a 6×6 connectivity matrix, C. Special cases of associative memory are the auto-association, where $x^i = y^i$ for all pairs i, and the hetero-association, where $x^i \neq y^i, i = 1, 2, \ldots$ (Palm, 1991). In Fig. 1(A) three associations are stored: $x^1 \rightarrow y^1, x^2 \rightarrow y^2$, and $x^3 \rightarrow y^3$. The resulting C matrix represents the three sets of paired events.

Recall of an input pattern is accomplished by multiplying the matrix C by a corresponding input pattern, e.g. $X^3 = (110100)$ and performing an integer division analogous to a variable threshold, the value of which is equal to the number of ones in the cueing pattern (i.e. $\theta = 3$). Perfect recall can be achieved by this division process even if the patterns share common active elements, provided that not too many different patterns have been presented (Fig. 1(B), (C)). Errors in recall will begin to occur as the matrix approaches saturation (Fig. 1(D)).

1.2. Hippocampus, neurons and threshold control

The hippocampus is one of the most widely studied brain regions, yielding a wealth of data on network architecture, cell types, the anatomy and membrane properties of pyramidal cells and interneurons, and synaptic plasticity (Andersen, Morris, Amaral, Bliss, & O'Keefe, 2007). Its basic functional role is hypothesized to be the temporary storage location of declarative memories (Andersen et al., 2007; Eichenbaum, Dunchenko, Wood, Shapiro, & Tanila, 1999; Wood, Dunchenko, & Eichenbaum, 1999).

* Corresponding author. Tel.: +44 1786 467422.
E-mail address: vcu@cs.stir.ac.uk (V. Cutsuridis).

0893-6080/$ – see front matter © 2009 Published by Elsevier Ltd
doi:10.1016/j.neunet.2009.07.009

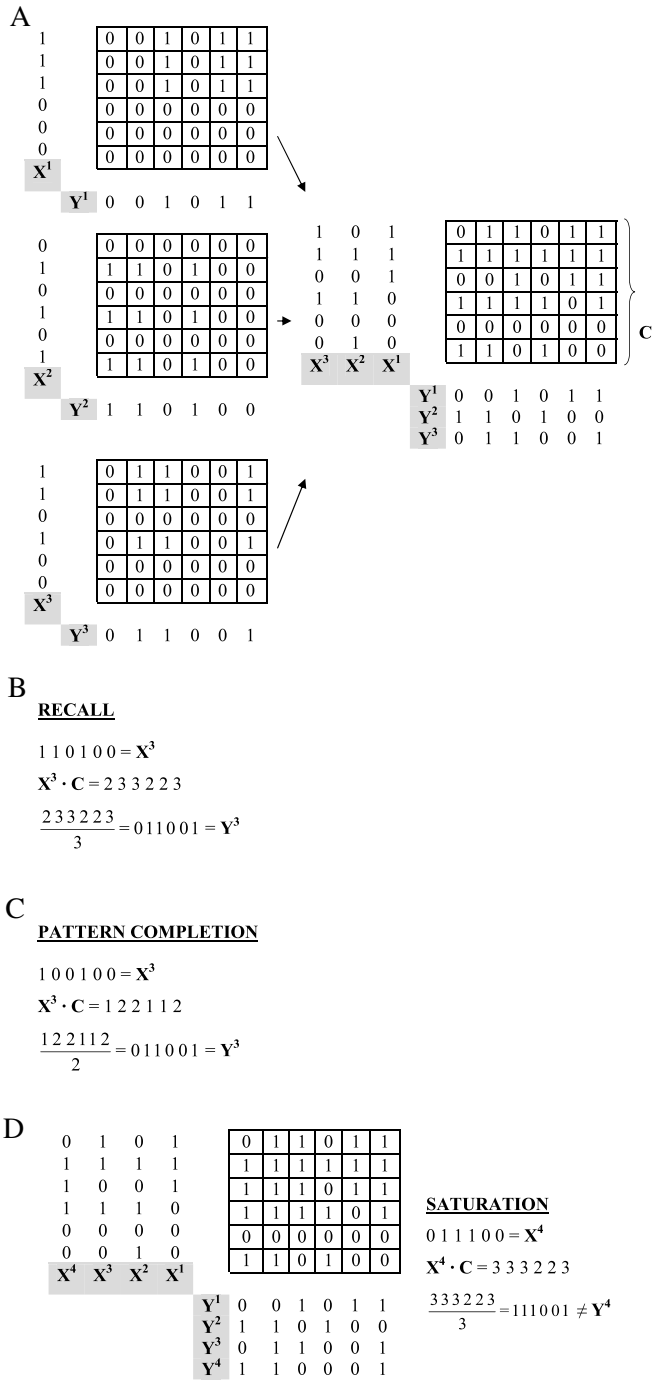

Fig. 1. (A) Associations of three memory patterns $X^1 \rightarrow Y^1$, $X^2 \rightarrow Y^2$, $X^3 \rightarrow Y^3$ using the mechanism of the correlation matrix. The resulting C matrix represents the three sets of paired events. (B) Perfect recall of an input pattern. (C) Pattern completion of an input pattern. (D) Saturation. Errors in recall start to occur as the matrix approaches saturation.

The hippocampal regions CA3 and CA1 have been proposed to be auto- and hetero-associators for the storage of declarative memories, respectively (Treves & Rolls, 1994).

Marr (1971, 1969) was the first to formulate a neural implementation of the correlation matrix hypothesis potentially supported by the hippocampus. His network consisted of N principal neurons, one inhibitory neuron and two types of inputs. All neurons were modeled as simple threshold neurons with resting threshold equal to one. Each of the Y inputs strongly depolarized a principal neuron and caused it to fire. All X inputs contacted all principal

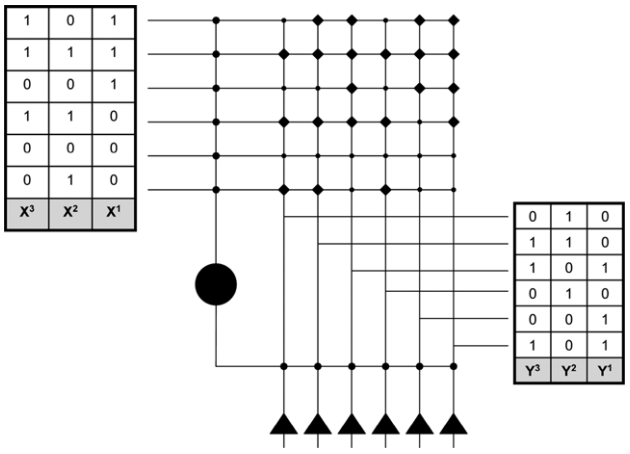

Fig. 2. Marr's neural implementation of the correlation matrix by the hippocampus (see Section 1.2 for details). Filled diamonds: active synapses (1); Filled circles: inactive synapses (0).

neurons. Their synaptic weights were initialized to zero and were strengthened according to a Hebbian rule. The X inputs also excited the inhibitory interneurons, which in turn inhibited the principal neuron's somata. The produced inhibitory signal was proportional to the total number of non-zero elements in the input pattern and performed a division operation in the principal neuron's soma, allowing this way the neurons that learned the pattern to recall it accurately. The system depicted in Fig. 2 is a subnet of Marr's network, which has stored the same set of paired associates as that of Fig. 1(A), and these can be recalled with the same accuracy.

Although Marr's model was a successful one in predicting that the hippocampus works like a content-addressable memory (CAM) system, it was also very rudimentary because the types of neurons used in this scheme were simple threshold neuronal nodes and the synaptic weights were updated according to an iterative time quantized update scheme, providing a very rough insight into the dynamical processes in the hippocampus. Since then, a dramatic accumulation of knowledge about the morphological, physiological and molecular characteristics, as well as the connectivity and synaptic properties of excitatory and inhibitory neurons in the hippocampus have been witnessed (Andersen et al., 2007). Excitatory neurons are primarily pyramidal neurons and they constitute 90% of all neurons in the hippocampus, whereas the remaining 10% are interneurons, primarily inhibitory, which are classified according to their morphological, physiological, molecular and synaptic characteristics into other numerous sub-classes (Somogyi & Klausberger, 2005). Collections of thousands of such cells then interact in cell assemblies (microcircuits), with each microcircuit being an individual machinery, which receives, processes and transmits information. In Section 2, we briefly review the experimental literature of the hippocampus regarding the different families of neurons and their operations in microcircuits and in rhythm generation. In Section 3, we review the various experimentally observed synaptic plasticity rules in the hippocampus. In Section 4, we review representative examples of simple and detailed spiking neuronal models of associative memory. Finally, in Section 5, we review some of the practical issues involved in biophysical modeling of microcircuits of associative memory and discuss future challenges.

2. Neuronal diversity, microcircuits and rhythms

In the hippocampus, diverse types of neurons form microcircuits and co-operate in time for the processing and storage of information. The dominant excitatory cell types in the hippocampal microcircuits are the pyramidal cell (PC), granule cell (GC) and

Please cite this article in press as: Cutsuridis, V., & Wennekers, T. Hippocampus, microcircuits and associative memory. Neural Networks (2009), doi:10.1016/j.neunet.2009.07.009

mossy cell (MC) (Andersen et al., 2007). These cells form networks which are the principal information processing structures in the hippocampus. Excitatory cells are also surrounded by a variety of GABAergic inhibitory interneurons (IN).

Neurons in the hippocampus receive external inputs via different pathways from the cortex and the extrahippocampal areas. In the dentate gyrus, GCs receive inputs directly from layer II of the entorhinal cortex (EC). In CA3, inputs come from the EC layer II to the distal apical tree of the PCs. Inputs to proximal and basal dendrites are largely from other CA3 PCs. Another excitatory input to CA3 comes from the GCs of the dentate gyrus, which form the mossy fiber synapses in the very proximal region of the apical tree of the PCs. In CA1, the Schaffer collateral excitatory input from the CA3 PCs impinges to PC proximal dendritic regions. Recurrent collaterals from other CA1 PCs synapse on the basal dendritic tree, whereas perforant path inputs from EC layer III reach the distal region of the apical dendritic trees of PCs.

Though a complete catalogue of IN types remains to be determined partly due to lack of a universally agreed nomenclature, the primary criterion for the classification of interneurons is the identity of postsynaptic targets. Based on this criterion, the interneurons can be divided into two classes: (1) perisomatic and (2) dendritic inhibitory cells. Several other sub-classes can be distinguished based on further anatomical, morphological, pharmacological (e.g. their neuropeptide or calcium-binding protein content) and physiological grounds (Ascoli, Alonso-Nanclares, Anderson, & Barionuevo, 2008). These include the perisomatic basket cells (BC) and axo-axonic cells (AAC) in dentage gyrus, CA3 and CA1, the dendritic bistratified cells (BSC) and oriens laconosum-moleculare cells (OLM) in the CA3 and CA1, and the molecular layer interneurons with axons in perforant-path termination zone (MOPP), the hilar interneurons with axons in perforant-path termination zone (HIPP), the hilar interneurons with axons in the commissural/associational pathway termination zone (HICAP), and the interneuron-selective cells (IS) in dentate gyrus (Morgan, Santhakumar, & Soltesz, 2007; Somogyi & Klausberger, 2005).

Inhibitory interneurons have been shown to innervate distinct regions of PCs, GCs and MCs as well as of other INs in the same area or across hippocampal areas via feedforward and feedback modes (Houser, 2007; Morgan et al., 2007; Somogyi & Klausberger, 2005). For example, axo-axonic cells innervate exclusively the axon-initial segment of pyramidal cells, granule cells and mossy cells, whereas basket cells innervate their cell bodies and proximal dendrites. Bistratified cells innervate the basal and oblique dendrites of CA3 and CA1 PCs and OLM cells target the apical dendritic tuft aligned with the entorhinal cortical input. HIPP cells synapse on the dendritic regions of GCs and MCs near the afferent inputs. MOPP cells feedforwardly inhibit granule cells, whereas HICAP cells inhibit the proximal GC dendrites, near where MC axons terminate and provide feedback inhibition. IS cells inhibit exclusively other interneurons and modulate the excitability and synchrony of the network. Long range INs, such as the somatostatin- and mGluR1α-positive neurons in stratum oriens project to the subiculum, other cortical areas and the medial septum, whereas somatostatin-negative ones and trilaminar cells project to the subiculum and other cortical areas but not to the septum (Jinno, Klausberger, Marton, & Dalezios, 2007; Klausberger & Somogyi, 2008; Morgan et al., 2007; Somogyi & Klausberger, 2005).

Inhibitory interneurons also display diverse firing patterns during network oscillations, which have different functional roles. (Klausberger & Somogyi, 2008). In the hippocampus, gamma frequency oscillations (30–80 Hz) constitute a basic clock cycle (Graham, 2003) and are embedded in theta frequency oscillations (4–10 Hz), which in turn control the phasing of storage and recall (Hasselmo, Bodelon, & Wyble, 2002). Sharp wave-associated ripples (100–200 Hz) occur during the offline replay and consolidation of previous experiences (Klausberger & Somogyi, 2008). In CA1, during sharp wave ripple oscillations, BCs and BSCs strongly increase their discharge rates in phase with the ripple episode. In contrast, axo-axonic cells fire before the ripple episode, but pause their activities during and after it. OLM cells pause their firings during ripples. On the other hand, during theta oscillations, OLM cells, BSCs and PCs increase their firing rates at the troughs of the extracellular theta, whereas BCs and AACs fire at the peaks of it. During gamma oscillations, the firing rates of BCs, AACs and BSCs correlate with the extracellular gamma in different degrees, whereas OLM cells do not correlate at all with gamma oscillations. An extensive review of different families of INs in the hippocampus, their properties and their firing patterns with respect to network oscillations can be found in Klausberger and Somogyi (2008).

Understanding the functional roles of these cells in encoding and retrieval of memories and rhythm generation currently poses a great challenge. Computational and mathematical models play an instrumental role in exploring such functions and facilitate the dissection of operations performed by the diverse interneurons. The aim of Section 4 is to provide a snapshot and a resumé of the current state-of-the-art of the ongoing research avenues concerning cortical microcircuits with particular emphasis on the functional roles of the various inhibitory interneurons in information processing in the hippocampus.

3. Synaptic plasticity rules and models

In 1949, Hebb postulated that the change in strength of a synapse is proportional to the product of both pre-synaptic and post-synaptic activity. In Hebbian learning a synapse is strengthened only when pre- and post-synaptic neurons are activated simultaneously (Hebb, 1949). This property of synaptic strengthening depends upon calcium influx through NMDA receptor channels, which are activated by a combination of presynaptic transmitter release, postsynaptic depolarization and back-propagating action potentials generated under certain experimental conditions in the cell body (Gerkin, Bi, & Rubin, in press). Synaptic plasticity can also be induced under certain conditions without the generation of postsynaptic action potentials (Lisman & Spruston, 2005).

Recently, Hebbian learning has been refined even further with the introduction of spike-timing dependent plasticity (STDP). In STDP, the precise timing of presynaptic and postsynaptic action potentials (spikes) determines the sign and magnitude of synaptic modifications (Bi & Poo, 1998; Markram, Lubke, Frotscher, & Sakmann, 1997). Bi and Poo (1998) showed that the profile of the STDP curve in the in-vitro hippocampal network has an asymmetrical shape with the largest LTP/LTD value at $\Delta\tau = t_{\text{post}} - t_{\text{pre}} = \pm 10$ ms, respectively. Since then several purely phenomenological (Morrison, Diesmann, & Gerstner, 2008) and biophysical models (Abarbanel, Gibb, Huerta, & Rabinovich, 2003; Karmarkar & Buonomano, 2002; Rubin, Gerkin, Bi, & Chow, 2005; Shouval, Bear, & Cooper, 2002) of STDP have been advanced.

Experimental evidence by Nishiyama, Hong, Mikoshiba, Poo, and Kato (2000) reported that "the profile of STDP induced in the hippocampal CA1 network with inhibitory interneurons is symmetrical for the relative timing of pre- and post-synaptic activation with two long-term depression (LTD) windows at ± 20 ms and a central long-term potentiation (LTP) peak at 0 ms". Further optical imaging studies revealed that the shape of the STDP profile depended on the location on the stratum radiatum (SR) dendrite. A symmetric STDP profile was observed in the proximal SR dendrite and an asymmetric STDP profile in the distal one (Aihara et al., 2007; Tsukada, Aihara, Kobayashi, & Shimazaki, 2005). Both STDP profiles have significant functional

Please cite this article in press as: Cutsuridis, V., & Wennekers, T. Hippocampus, microcircuits and associative memory. Neural Networks (2009), doi:10.1016/j.neunet.2009.07.009

implications in associative learning. The symmetric STDP profile plays a role in the 25 ms coincidence window (roughly a gamma cycle) for heteroassociation in the perforant path and Schaffer collateral inputs in CA1 neurons, whereas the asymmetric STDP profile may play a role in sequence learning (Aihara et al., 2007). Furthermore, it has been reported that the switch between modes of operation (symmetry vs. asymmetry) is due to the presence of $GABA_A$ inhibition in the proximal SR dendrites (Aihara et al., 2007).

In a recent biophysical modeling study by Cutsuridis, Cobb, and Graham (2008b) the effects of $GABA_A$ on this switch of operation in the CA1 dendrites were quantitatively investigated. They showed that that the switch is indeed due to $GABA_A$ depletion and it depends on the $GABA_A$ conductance value, the frequency of $GABA_A$ input presentation (theta vs. gamma), the relative timing of the inhibitory input with the pre- and post-synaptic activations and the burst interspike interval (Cutsuridis et al., 2008b; Cutsuridis, Cobb, & Graham, 2008c, 2009b; Cutsuridis, Graham, & Cobb, 2009c; Cutsuridis, Cobb, & Graham, 2009d). In addition and in contrast to the experimental evidence (Aihara et al., 2007; Nishiyama et al., 2000; Tsukada et al., 2005), the simulated symmetrical STDP curve was centered at +10 ms ($\Delta\tau = t\text{post} - t\text{pre} > 0$) and not at 0 ms and the two distinct LTD tails were present at −10 ms and +40 ms and not at ±20 ms. Similar results have been produced experimentally by Wittenberg and Wang (2006).

4. Computational network modelling

4.1. Spiking neuronal models

Sommer and Wennekers (2000, 2001) advanced a spiking neural network model as an extension to the original hippocampal CAM model (Marr, 1971; Palm, 1980; Willshaw et al., 1969) to investigate its memory capacity and robustness of efficient retrieval under varying memory load and type of external stimulation (tonic and pulsed). In the model, neurons were modelled as two compartmental (soma and dendrite) Pinsky and Rinzel spiking neurons consisting of a wealth of ionic currents. For learning they used the clipped synaptic modification rule of the Willshaw et al. model (1969). All cells were recurrently connected and their connectivity depended on the number and size of the stored patterns. Memory patterns were sequences of binary numbers (1 or 0) with ten 1 s per pattern. Each pattern was presented to a fixed number of cells in the network and each cell was active in more than one memory pattern. AMPA and NMDA excitation was present on the dendrites, whereas GABA-A inhibition acted on the soma. Inhibition worked as a global non-constant threshold, which was proportional to the instantaneous ensemble firing activity of the principal cells. With tonic stimulation, the addressed memory was an attractor of the network dynamics. The memory was displayed rhythmically, coded by phase-locked bursts or regular spikes. The participating neurons had rhythmic activity in the gamma-frequency range (30–80 Hz). If the input was switched from one memory to another, the network activity followed this change within one or two gamma cycles. On the other hand, with pulsed stimulation, memories were not attractors. Memory patterns were retrieved within one or two gamma cycles. With pulsed stimulation, bursts became relevant for coding and their occurrence could be used for discriminating related processes from background activity.

Recently, Hunter, Cobb, and Graham (2008a, 2008b) compared and contrasted the performance of the Sommer and Wennekers model (2000) with the previously published recall results of the Willshaw model (Graham & Willshaw, 1995, 1997). They tested how well the network can recall a pattern when there is partial connectivity or corruption due to noise (possibly by overlap in pattern storage) and how the global GABA-A inhibition of the Sommer and Wennekers model could implement the winner-take-all (WTA) recall of a stored pattern. Briefly, the WTA approach decides which output units should fire based on the weighted (dendritic) sum of their inputs. Hence, WTA chooses the required number of units with the highest dendritic sum to fire during pattern recall. Pattern connectivity complicates recall as a neuron cannot distinguish between missing physical connections and connections that have not been modified during storage.

Recall was tested by tonically stimulating 5 from a known pattern of 10 pyramidal cells using an injected current to either the soma or the dendrite with a varying strength. Biophysical implementations of three separate WTA recall methods were used: (1) Standard WTA implemented by intrinsic PC thresholding (increases in Na^+ density and membrane resistance) and global inhibition; (2) Normalized WTA implemented by localized inhibition proportional to the excitation a cell could receive, the range of EPSPs and the dendritic sums produced; and (3) amplified WTA via a non-linear increase of EPSP summation, so that the cells that reached a certain membrane potential increased their summed EPSP amplitude via a persistent Na^+ current. Recall performance was tested by storing 50 random patterns, each consisting of 10 active cells, in the network and then using 5 of the 10 cells of a stored pattern as a recall cue. Physical connectivity was set to 100% or 10%. Recall quality in 10% connectivity was: (1) 61% in standard WTA, (2) 64% in normalized WTA and (3) 65% in amplified WTA.

4.2. Detailed spiking neuronal models

In this section, we will focus only on detailed biophysical network models consisting of excitatory neurons and numerous sub-classes of inhibitory interneurons and discuss their functional roles in the storage and recall processes. Menschik and Finkel (1998) advanced a network model of hippocampal CA3 region dynamics inspired by the Buzsaki "two-stage" memory model and the suggested role for interneurons (Buzsaki, 1989; Buzsaki & Chrobak, 1995) and the Lisman and colleagues model on embedded gamma cycles within the theta rhythm (Lisman, 2005; Lisman & Idiart, 1995). They used detailed biophysical representations of multi-compartmental models of pyramidal cells and two types of inhibitory interneurons: basket cells and chandelier cells to study the modulation and control of storage and recall dynamics in Alzheimer's disease by subcortical cholinergic and GABAergic input to the hippocampus. They showed that synchronization in the gamma frequency range can implement an attractor based auto-associative memory, where each new input pattern that arrives at the beginning of each theta cycle comprised of 5–10 embedded gamma cycles drives the network activity to converge over several gamma cycles to a stable attractor that represents the stored memory. Their results supported the hypothesis that spiking and bursting in CA3 pyramidal cells mediate separate behavioural functions and that cholinergic input regulates the transition between behavioural states associated with the online processing and recall of information. Cholinergic deprivation led to the slowing of gamma frequency, which reduced the number of "gamma cycles" within the theta rhythm available to reach the desired attractor state (i.e. memory loss and cognitive slowing seen in AD).

Kunec, Hasselmo, and Kopell (2005) advanced a detailed CA3 model of the hippocampus using biophysical representations of the major cell types including pyramidal cells (PC) and two types of interneurons to dissect the operations performed by the various types of interneurons in and inputs to the network as well as investigate how variations in biophysically meaningful and experimentally measurable parameters affect the simulated encoding and retrieval. Their network consisted of 5

Please cite this article in press as: Cutsuridis, V., & Wennekers, T. Hippocampus, microcircuits and associative memory. Neural Networks (2009), doi:10.1016/j.neunet.2009.07.009

PC, 1 inhibitory oriens-lacunosum-moleculare (OLM) interneuron and a population of inhibitory basket cells. The pyramidal cell was a 4-compartment cell, whereas all other cells were single compartmental. All PC cells were all-to-all coupled, mimicking the extensive recurrent collateral system of CA3. Each PC received somatic inhibition from the population of basket cells, proximal excitation from the dentate gyrus, mid-dendritic excitation from other pyramidal cells, distal inhibition from OLM cells and distal excitation from direct entorhinal cortical input. OLM cells received excitatory input from the PCs and inhibitory input from the basket cells. The basket cells received excitatory inputs from the PC and inhibitory input from the septal input. Inputs to the network came from the medial septum, which paced the theta rhythm in the CA3 model into two half sub-cycles (one for storage and the other one for recall), and the entorhinal cortex (directly and via the dentate gyrus). Their model reproduced experimental results showing that the various cell types fire at a preferred phase relationship with respect to the underlying theta rhythm and to each other and that they indeed have distinct roles in storage and recall of memory patterns.

Cutsuridis, Hunter, Cobb, and Graham (2007), Cutsuridis, Cobb, and Graham (2008a), Graham and Cutsuridis (2009) recently advanced a far more detailed biophysical model of the CA1 microcircuit of the hippocampus in order to investigate several questions in dependence of various model properties like memory pattern load and input pattern presentation periods. They investigated: (1) how storage and recall are controlled in the CA1 microcircuit? (2) What roles do the various types of inhibitory interneurons play in the dynamical CA1 information processing? And (3) What is the recall performance of the network as a function of input pattern loading and presentation frequency? Their network consisted of 100 pyramidal cells (P), 2 basket cells (B), 1 axo-axonic cell (AA), 1 bistratified cell (BS) and 18 OLM cells (see Fig. 3). The neuronal diversity, morphology, ionic and synaptic properties, connectivity and spatial distribution followed closely known experimental evidence of the hippocampal circuitry (see Cutsuridis et al. (2008a) for details). Excitatory inputs (random sequences of zeros and ones repeatedly applied every $\Delta\tau = 5$ ms or 7 ms or 8 ms or 10 ms or 11 ms were present throughout the storage and recall sub-cycles) and inhibitory inputs (random sequences of zeros and ones repeatedly applied every $\Delta\tau = 5$ ms or 7 ms or 8 ms or 10 ms or 11 ms were present during the recall sub-cycle only) to the network came from the entorhinal cortex (EC), the CA3 Schaffer collaterals and the medial septum. The EC input provided the sensory information, whereas all other inputs provided context and timing information. Storage was accomplished via an STDP learning rule applied at the P AMPA SR synapses, where the pre-synaptic CA3 Schaffer collateral input was compared with the amplified postsynaptic P SR voltage response. During recall, the P AMPA synaptic conductance was equated to the conductance value at the end of the storage cycle *plus* a constant term, which represented the lift-off of a cyclical theta presynaptic $GABA_B$ inhibition (Molyneaux & Hasselmo, 2002) to the CA3 Schaffer collaterals that was present during storage.

The model demonstrated the biological feasibility of the separation of storage and recall processes into separate theta sub-cycles (Hasselmo et al., 2002). Based on experimental evidence that has shown that the conduction latency of the EC layer III input to CA1 P cell LM dendrites is less than 9 ms (ranging between 5–8 ms), whereas the conduction latency of the EC layer II input to CA1 P cell SR dendrites via the di/tri-synaptic path is greater than 9 ms (ranging between 12–18 ms) (Leung, Roth, & Canning, 1995; Soleng, Raastad, & Andersen, 2003), the model predicted that the only way EC and CA3 input patterns could be hetero-associated in CA1 SR dendrites is by the careful timing between the incoming presynaptic CA3 Schaffer collateral spikes and the amplified due to the incoming EC input postsynaptic voltage response in the proximal P SR dendrites. The amplification of the P SR dendritic signal was due to the activated, by the strong hyperpolarization from the B and AA inhibition of the soma and axon, non-specific cationic *h*-channels, which allowed the influx of Na^+, in the P SR dendrites and soma and hence the "boosting" of the postsynaptic voltage response in the proximal P SR dendrites.

The model predicted that the only way such careful timing can take place if inhibitory cells are switched on and off in certain phase relationships with respect to the theta cycle, as demonstrated by recent experimental data (Klausberger et al., 2003, 2004). More specifically, the model predicted that during storage the AAs and Bs are switched on and operate to: (1) exert tight inhibitory control on the axons and somas of the pyramidal cells, thus preventing them from firing during the storage cycle (Klausberger et al., 2003), (2) exert powerful inhibitory control to neighboring basket cells and to bistratified cells, which prevents the latter from firing during the storage cycle (Klausberger et al., 2004) and disrupting the learning process, and (3) maintain the environment necessary for the generation of non-specific Na^+ based cation *h*-channels and subsequently the enhanced postsynaptic response in the P SR dendrites. During recall, the model predicted that the septal inhibition is switched on, which in turn inhibits the AAs and Bs, which disinhibit the BSs and allow the Ps to fire action potentials and hence recall the information. BSs provide a general broadcasting inhibitory signal to all Ps, which silences all spurious cells in the network and allows cells that have learned the pattern to recall it. Finally, OLM cells are switched on during recall by the P excitation (Klausberger et al., 2003, 2004) and inhibit the P apical dendritic tuft, thus preventing unwanted or similar memories from being recalled.

The recall performance of the model (see Fig. 4) for an input pattern was tested for different input pattern presentation periods ($\Delta\tau = 5$ ms, 7 ms, 8 ms, 10 ms and 11 ms), levels of cue (EC input) loading (10%, 50% and 75% of the cue was presented to P cells) and learning paradigms (one-trial paradigm vs. many-trials paradigm). To estimate the recall performance, the cells, which belonged to the pattern and were active during the retrieval cycle were counted and divided by the required ones. If the active cells were equal to the required ones, then the recall fraction was 1 (i.e. perfect recall). At 75% pattern loading, the recall performance for "many-trials" learning paradigm was nearly perfect (100%) regardless of the presentation period with the exception at 7 ms (95%). At 50% and 10% pattern loading for the "many-trials" learning paradigm, the recall performance dropped by 5% and 20% respectively when the input presentation period was 5 ms. At larger input presentation periods, the recall performance degraded progressively for both 50% and 10% pattern loading reaching a minimum of 45% and 70% respectively at 11 ms.

In the "one-trial" paradigm at 75% pattern loading, the recall performance across input presentation periods varied slightly between 60%–80% (unpublished simulation results of our group). At 50% and 10% pattern loading, the recall performance dropped at 65% and 55% respectively at 5 ms (unpublished simulation results of our group). Across input presentation periods, the recall performance at 50% pattern loading varied between 45% and 65%, whereas at 10% pattern loading varied between 20% and 55% (unpublished simulation results of our group).

Across learning paradigms at 75% pattern loading and 5 ms time input presentation period, a drop of 20% in recall performance was observed between the "many-trial" and "one-trial" learning paradigms. Across all other presentation periods, the recall performance drop varied from 20% (7 ms) to 40% (8 ms) between the two paradigms. A constant 30% drop was observed across all presentation periods at 50% pattern loading between the two paradigms with the exception of a 10% increase at 11 ms during the one-trial learning paradigm. At 10% pattern loading, the recall performance drop between the "many-trials" and the "one-trial" paradigms varied from 25% (5 ms) to 50% (8 ms and 11 ms).

Please cite this article in press as: Cutsuridis, V., & Wennekers, T. Hippocampus, microcircuits and associative memory. Neural Networks (2009), doi:10.1016/j.neunet.2009.07.009

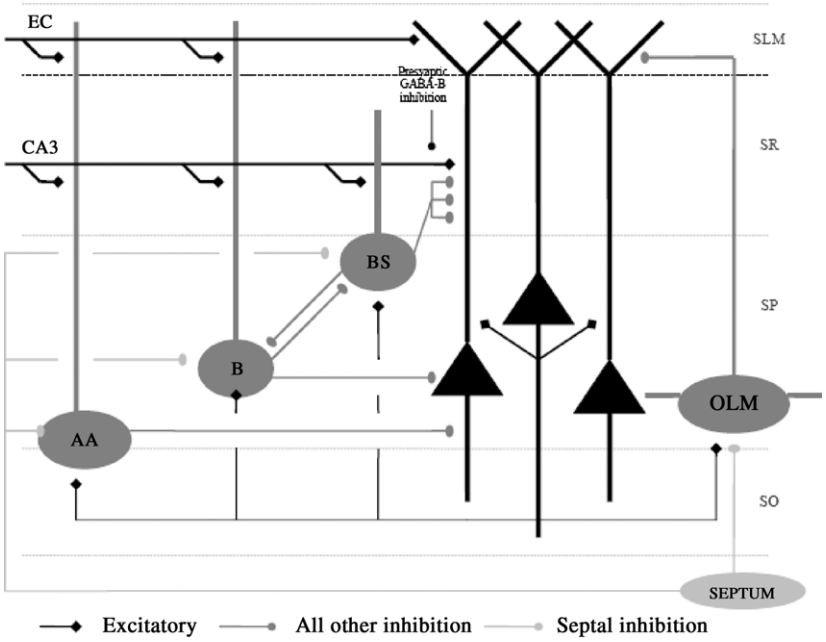

Fig. 3. Hippocampal CA1 microcircuit showing major cell types and their connectivity. Black filled triangles: pyramidal cells. Dark gray filled circles: CA1 inhibitory interneurons. EC: entorhinal cortex input; CA3: CA3 Schaffer collateral input; AA: axo-axonic cell; B: basket cell; BS: bistratified cell; OLM: oriens lacunosum-moleculare cell; SLM: stratum lacunosum moleculare; SR: stratum radiatum; SP: stratum pyramidale; SO: stratum oriens. Light gray filled circles: Septal GABA inhibition.

Finally, further unpublished simulations from our group investigated how different local circuits within the CA1 microcircuit can remove spurious activity and lead to the good recall performance. Spurious activity is defined as the activity of a cell that is not part of the group of cells which encoded the input pattern. Spurious activity can corrupt the recall of a memory episode, as a similar memory, but not the true one will be recalled. For example, if our task is the recall of our grandmother sitting by the fireplace by herself, then spurious activity can falsely co-activate cells encoding the grandson memory, and so our recalled memory episode will include the grandmother *with* her grandson by the fireplace. In the model, during recall only the pyramidal, bistratified and OLM cells were active (Klausberger et al., 2003, 2004). The role of the bistratified cells was to set the threshold, so that only the pyramidal cells that have learned the pattern remained active, whereas all others were silenced. Two modes of inhibitory action control sufficient for removing the spurious activity were investigated: (1) Feedforward GABA-A and GABA-B bistratified cell inhibition to pyramidal cells, without feedback excitation from the pyramidal cell to bistratified cells, and (2) Feedforward GABA-A bistratified cell inhibition to pyramidal cells with feedback excitation from the pyramidal cell to bistratified cells.

Pyramidal cells' spike responses in mode 1 across the storage and recall phases for various GABA-A and GABA-B synaptic strengths are depicted in Fig. 5. When there is no bistratified cell inhibition, then the CA3 input is sufficient to excite all P cells in the network (top). As soon as the bistratified cell $GABA_A$ inhibition ($g_{GABAA} = 0.004$ mS/cm^2) is turned on (middle), then some of the spurious activity is removed. For strong $GABA_A$ and $GABA_B$ bistratified cell inhibition (bottom) ($g_{GABA-A} = 0.006$ mS/cm^2, $g_{GABA-B} = 0.004$ mS/cm^2), nearly all spurious activity is removed, allowing only the most active cells from the pattern (15 out of 20) to exceed the threshold and remain active. This is due to the fast kinetics of feedforward $GABA_A$ inhibition, which eliminate the spurious activity from the early gamma cycles, whereas the $GABA_B$ inhibition cleans the spurious activity from the later gamma cycles, due to its slower kinetics.

Pyramidal cells' spike response in the presence of only feedforward $GABA_A$ ($g_{GABA-A} = 0.01$ mS/cm^2) bistratified cell inhibition to pyramidal cell and feedback excitation from the pyramidal cell to bistratified cells is depicted in Fig. 6. $GABA_B$ was absent in these simulations. Similar results were yielded as in mode 1 (16 out of 20 cells from the pattern were active). As before the feedforward $GABA_A$ inhibition alone will eliminate the early spurious activity, but leave the spurious activity from the late gamma cycles. Now recurrent excitation will drive the bistratified cells into a repetitive spiking mode that will "clean" any unwanted late gamma cycle spurious activity.

Recently, Cutsuridis, Cobb, and Graham (2009a) extended the CA1 microcircuit model (Cutsuridis et al., 2008a) to test: (1) What is the recall performance of new and previously stored patterns in the presence and absence of various types of inhibitory interneurons? And (2) What is the mean recall quality of the CA1 microcircuit as the number of stored patterns increases? The CA1 microcircuit model (Cutsuridis et al., 2008a) was extended in the following ways:

1. Simplified morphologies were used for all cells.
2. The amplification of the postsynaptic PC SR voltage response due to the non-specific I_h current was no longer considered.
3. A medium afterhyperpolarization (AHP) current was included in the SR dendrites to induce Ca^{2+} spikes.
4. During storage, the P AMPA synaptic conductance was equated to a fraction of the recall cycle conductance value, which represented the presence of a cyclical theta presynaptic $GABA_B$ inhibition to the CA3 Schaffer collaterals (Molyneaux & Hasselmo, 2002).
5. The EC perforant path and CA3 Schaffer collateral inputs were repeated throughout the storage and recall cycles every 20 ms and 25 ms, respectively, and not every $\Delta\tau$ as in Cutsuridis et al. (2008a).
6. Learning of new patterns was based on the variant of the STDP learning rule, which during storage the weights were not allowed to grow indefinitely, but were bounded by w_{max}. As in Cutsuridis et al. (2008a), STDP was on during the storage cycle and off during the recall one and storage was based on the forward pairing of the EC perforant path and the delayed by 10 ms CA3 Schaffer collateral input.

Please cite this article in press as: Cutsuridis, V., & Wennekers, T. Hippocampus, microcircuits and associative memory. Neural Networks (2009), doi:10.1016/j.neunet.2009.07.009

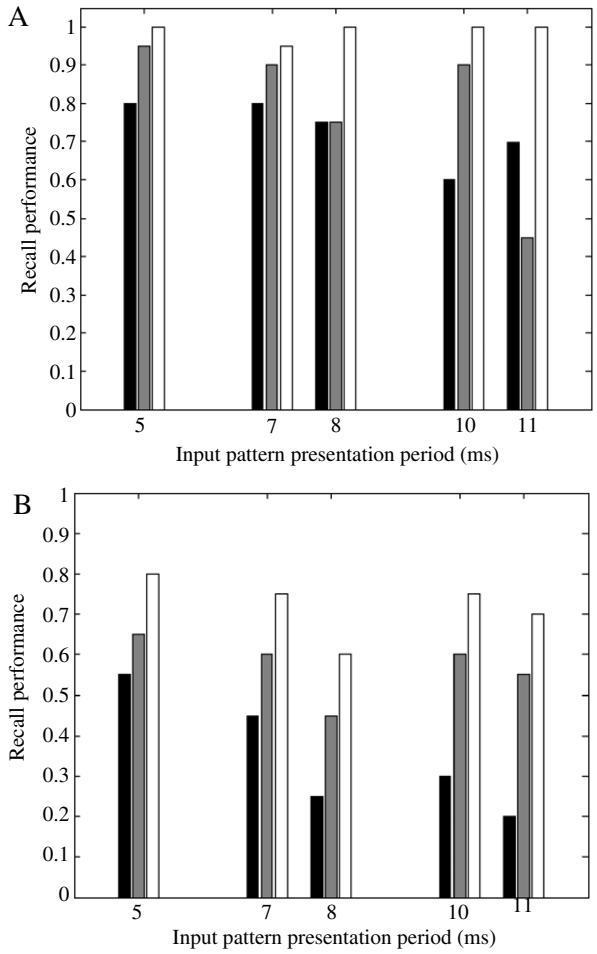

Fig. 4. Bar graph of recall performance of first recalled pattern vector as a function of input pattern presentation period. (A) Many-trials learning paradigm (reproduced with permission from Cutsuridis et al. (2008c), Figure 3, p. 244, Copyright© Springer-Verlag). (B) One-trial learning paradigm (unpublished simulations from our group). *Black bar*: 10% cue completion. *Gray bar*: 50% cue completion. *White bar*: 75% cue completion.

7. The CA3-to-CA1 P connection weight matrix was not randomly initialized close to zero as in Cutsuridis et al. (2008a) and allowed to grow towards the nearly perfect recall set of weight values, but instead, the CA3-to-CA1 P connection weight matrix was initialized near the nearly perfect recall set of weight values using an external weight matrix generated according to a clipped Hebbian learning rule and either tested the recall performance of already stored patterns in the presence/absence of the inhibitory interneurons or the storage of new patterns as perturbations from the latter set of weight values.
8. Recall performance was measured using the normalized dot product metric.

The new model predicted that during storage, the presence of the pre-synaptic $GABA_B$ suppression of feedforward CA3 synaptic input to CA1 is required to prevent interference from previously stored associations leading to excessive weight strengthening (see Figure 15d in Cutsuridis et al. (2009a)). An additional mechanism was the B and AA inhibition, which during storage contributed to hyperpolarizing pattern and non-pattern pyramidal cells and hence prevented the former from firing and information from "leaking out" and the latter from learning the pattern.

Also, the new model predicted that the STDP rule can store a new pattern, as determined by EC inputs, in association with a CA3 input pattern provided (a) EC and CA3 inputs are repeatedly presented such that the "next" EC input arrives within the STDP

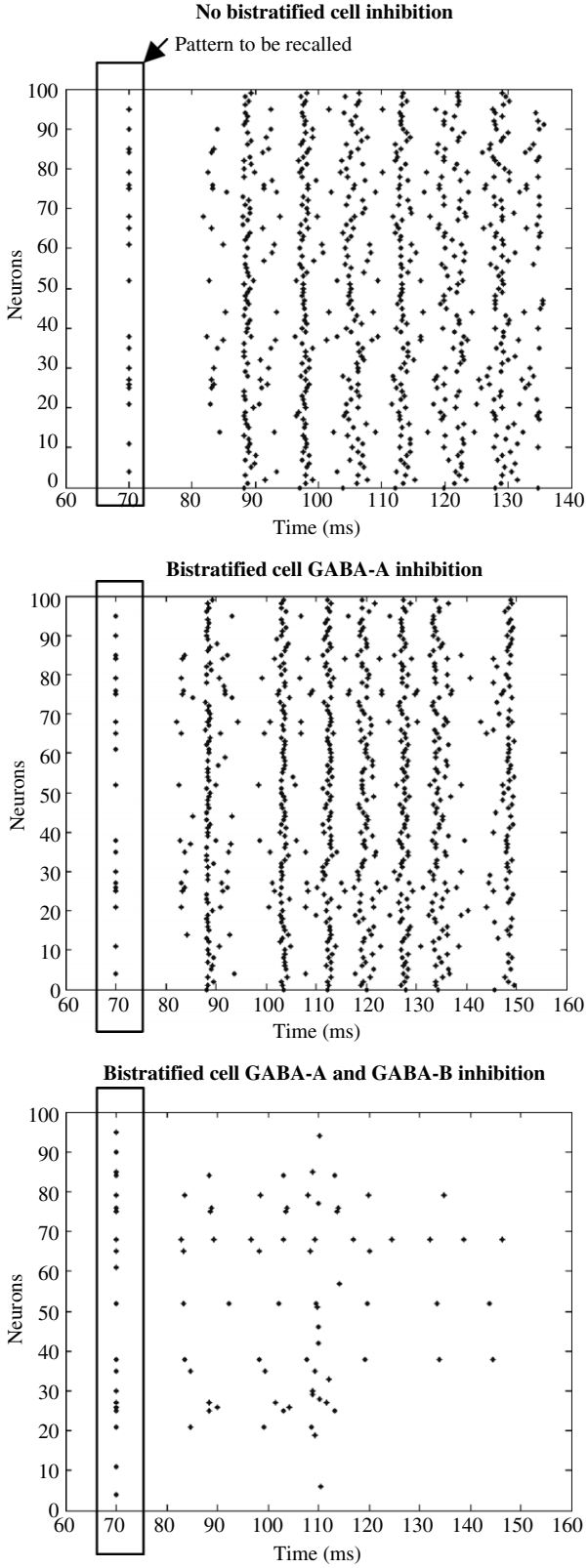

Fig. 5. Spike raster plots of all network pyramidal cells in the (*Top*) absence of bistratified inhibition, (*Middle*) presence of bistratified GABA-A inhibition ($g_{GABA-A} = 0.004$ mS/cm^2), (*Bottom*) presence of bistratified GABA-A *and* GABA-B inhibition ($g_{GABA-A} = 0.006$ mS/cm^2, $g_{GABA-B} = 0.004$ mS/cm^2). Spike vector inside parallelogram is the desired input pattern vector to be recalled. Spikes at 70 ms are included only for illustration purposes.

LTP time window following a CA3 input, and (b) LTD is not too strong since, due to transmission delays, an EC input will always

Please cite this article in press as: Cutsuridis, V., & Wennekers, T. Hippocampus, microcircuits and associative memory. Neural Networks (2009), doi:10.1016/j.neunet.2009.07.009

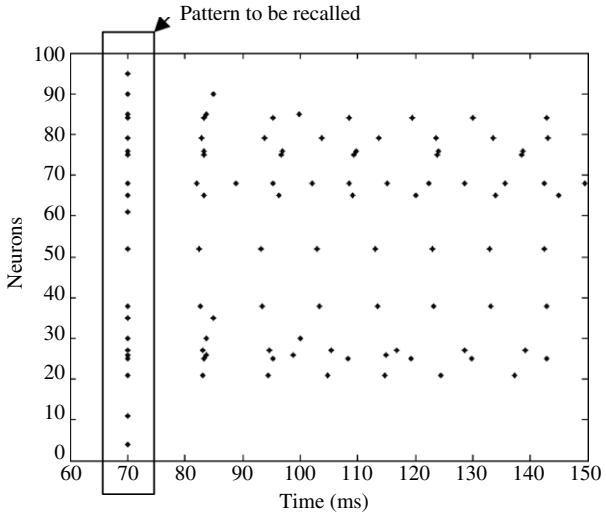

Fig. 6. Spike raster plot of all network pyramidal cells in the presence of *only* bistratified GABA-A inhibition ($g_{GABA-A} = 0.01$ mS/cm^2). Spike vector inside parallelogram is the desired input pattern vector to be recalled. Spikes at 70 ms are included only for illustration purposes.

arrive within the STDP LTD time window preceding a CA3 input (based on the assumption that the layer II and layer III EC cells fire in phase with each other).

Finally, the model predicted that during recall, inhibition from BSs was needed for accurate recall of a previously stored pattern by contributing to the thresholding of pyramidal cell firing (see Figure 11 in Cutsuridis et al. (2009a)), whereas OLM inhibition was effective at removing spurious EC input that may distort pattern recall (see Figure 13 in Cutsuridis et al. (2009a)).

5. Practical issues and future challenges

It is clear that large scale biophysical models of associative memory are very important, because they allow us to run in-silico experiments of networks of neurons, while bypassing the technical difficulties of a real experiment, and investigate questions related to the interaction between the local microcircuit activity and global processing to achieve the desired overall processing functionality observed in learning and memory. To construct such detailed biophysical large scale models, though, several practical issues such as parameter searching, network scaling, suitable simulation environments, and computational speed and efficiency need to be addressed.

Microcircuit models often require tweaking of tens or hundreds of parameters. These parameters are often laboriously hand-tuned using information from anatomical and physiological studies, including morphological parameters, ionic and synaptic conductances and reversal potentials of single neurons, numbers of different neuronal subtypes, and connection probabilities between different types of neurons. Unfortunately, for most neurons, most anatomical and physiological studies don't focus on providing such quantitative data and hence this type of information is not described in sufficient detail. For these reasons, computational modelers resort in using ad-hoc parameter values and ranges of them not found in experimental studies.

An attractive alternative is the use of advanced optimization techniques such as brute-force methods, simulated annealing, genetic algorithms, evolution strategies, differential evolution and particle-swarm optimization that make parameter searches automatic (Hasselmo & Kapur, 2000; Van Geit, de Schutter, & Archard, 2008). Free commercial software packages as Neurofitter combine a phase–plane trajectory density fitness function with several search algorithms (Van Geit et al., 2008).

Detailed simulations of entire mammalian brain regions with the same number and types of neurons as in the real brain, the same neuronal morphology (length and diameter), ionic and synaptic conductances, and connection probabilities between them are not currently possible. Simulations of such large networks would require too much time and too much memory to be practical. Thus, anyone interested in large scale microcircuit simulations must be faced with the problem of scaling down the size of the network and using oversimplified models of real neurons with reduced morphology, ionic and synaptic properties and extrinsic and intrinsic connectivity. If a microcircuit is only reduced in size without scaling down the connection probability or connections strength of its cellular components, then cells might never receive sufficient synaptic input to go over the threshold. Potential solutions to this problem are the increase of the percentage connectivity between individual units in the network or the increase of the synaptic strength of neuronal connections. These changes need to be made with great care as a decrease in the number of synapses below a certain value can change dramatically the dynamical properties of the network (Hasselmo & Kapur, 2000).

A number of suitable simulation environments for the development of networks of spiking neurons are currently available, e.g. NEST, NeoCortical Simulator (NCS), Circuit simulator (CSIM), XPPAUT, SPLIT, Catacomb, Hippo-Surf, MCell and neuroConstruct, GENESIS and NEURON are also some of them (Brette, Rudolph, Carnevale, & Hines, 2007; Gleeson, Steuber, & Silver, 2007) The GENESIS and NEURON simulation packages are the most popular ones. They are scripting languages with extensive build-in functions focused on the implementation of realistic multicompartmental neurons and networks thereof. Both GENESIS and NEURON have been parallelized and hence simulation speed has been greatly enhanced. Parallel versions of GENESIS (PGENESIS) and NEURON can run on almost any parallel cluster, supercomputer, or network of workstations where the message passing protocol (MPI) is supported.

Finally, constructing a detailed microcircuit model with tens or hundred of parameters, scaling it down and finding a suitable simulation environment to simulate it most of the times is not enough as its speed and performance greatly depends on computer speed. Supercomputers and clusters of them may offer ultra-fast computer speed that can be used for large scale computer simulations in a wide range of fields including computational neuroscience. Speeds that can reach up to 10 petaflops (10^{16} floating-point operations per second) may be very helpful. Such next generation supercomputers are currently been developed all over the world (see "Brain and Neural Systems Team of the Integrated Life Simulation Project", http://www.nsc.riken.jp/project-eng.html, (2008)).

Acknowledgements

VC was supported by the EPSRC project grant EP/D04281X/1. TW was supported by the EPSRC project grant EP/C010841/1.

References

Abarbanel, H. D. I., Gibb, L., Huerta, R., & Rabinovich, M. I. (2003). Biophysical model of synaptic plasticity dynamics. *Biological Cybernetics*, *89*, 214–226.

Aihara, T., Abiru, Y., Yamazaki, Y., Watanabe, H., Fukushima, Y., & Tsukada, M. (2007). The relation between spike-timing dependent plasticity and Ca2+ dynamics in the hippocampal CA1 network. *Neuroscience*, *145*, 80–87.

Andersen, P., Morris, R., Amaral, D., Bliss, T., & O'Keefe, J. (2007). *The hippocampus book*. Oxford: University press.

Ascoli, G. A., Alonso-Nanclares, L., Anderson, S. A., Barionuevo, G., et al. (2008). Petilla terminology: Nomenclature of features of GABAergic interneurons of the cerebral cortex. *Nature Reviews Neuroscience*, *9*(7), 557–568.

Bi, G. Q., & Poo, M. M. (1998). Synaptic modifications in cultured hippocampal neurons: Dependence on spike timing, synaptic strength and postsynaptic cell type. *Journal of Neuroscience*, *18*, 10464–10472.

Brette, R., Rudolph, M., Carnevale, T., Hines, M., et al. (2007). Simulation of networks of spiking neurons: A review of tools and strategies. *Journal of Computational Neuroscience*, *23*(3), 349–398.

Buzsaki, G. (1989). Two-stage model of memory trace formation: A role for noisy brain states. *Neuroscience*, *31*, 551–570.

Buzsaki, G., & Chrobak, J. J. (1995). Temporal structure in spatially organized neuronal assembles: A role for interneuronal networks. *Current Opinion Neurobiology*, *5*, 504–510.

Cutsuridis, V., Hunter, R., Cobb, S., & Graham, B. P. (2007). Storage and recall in the CA1 microcircuit of the hippocampus: A biophysical model. In *BMC neuroscience*: *Vol. 8. Sixteenth annual computational neuroscience meeting CNS*2007* (p. P33). (Suppl 2).

Cutsuridis, V., Cobb, S., & Graham, B. P. (2008a). Encoding and retrieval in a CA1 microcircuit model of the hippocampus. In V. Kurkova, R. Neruda, & J. Koutnik (Eds.), *LNCS*: *Vol. 5164. ICANN 2008* (pp. 238–247). Berlin, Heidelberg: Springer-Verlag.

Cutsuridis, V., Cobb, S., & Graham, B. P. (2008b). A Ca2+ dynamics model of the STDP symmetry-to-asymmetry transition in the CA1 pyramidal cell of the hippocampus. In V. Kurkova, R. Neruda, & J. Koutnik (Eds.), *LNCS*: *Vol. 5164. ICANN 2008* (pp. 627–635). Berlin, Heidelberg: Springer-Verlag.

Cutsuridis, V., Cobb, S., & Graham, B. P. (2008c). A CA1 heteroassociative microcircuit model of the hippocampus. In *ARIADNE: Research in encoding and decoding of neural ensembles*.

Cutsuridis, V., Cobb, S., & Graham, B. P. (2009a). Encoding and retrieval in the hippocampal CA1 microcircuit model. *Hippocampus*, doi:10.1002/hipo.20661.

Cutsuridis, V., Cobb, S., & Graham, B. P. (2009b). How bursts shape the STDP curve in the presence/absence of GABA inhibition. In *Proceedings of the 19th international conference on artificial neural networks*.

Cutsuridis, V., Graham, B. P., & Cobb, S. (2009c). Modelling the effects of GABA-A inhibition on the spike timing dependent plasticity (STDP) of a CA1 pyramidal cell. In *18th annual computational neuroscience meeting CNS*2009*.

Cutsuridis, V., Cobb, S., & Graham, B. P. (2009d). Modelling the STDP symmetry-to-asymmetry transition in the presence of GABAergic inhibition. *Neural Network World*.

Eichenbaum, H., Dunchenko, P., Wood, E., Shapiro, M., & Tanila, H. (1999). The hippocampus, memory and place cells: Is it spatial memory or a memory of space? *Neuron*, *23*(2), 209–226.

Gerkin, R. C., Bi, G. Q., & Rubin, J. E. (2010). A phenomenological calcium based model of STDP. In V. Cutsuridis, B. P. Graham, S. Cobb, I. Vida (Eds). *Hippocampal microcircuits: A computational modeller's resource book*, New York, USA; Springer (in press).

Gleeson, P., Steuber, V., & Silver, R. A. (2007). Neuro construct: A tool for modeling networks of neurons in 3D space. *Neuron*, *54*(2), 219–235.

Graham, B. P. (2003). Dynamics of storage and recall in hippocampal associative memory networks. In P. Erdi, A. Esposito, M. Marinaro, & S. Scarpetta (Eds.), *Computational neuroscience: Cortical dynamics* (pp. 1–23). Berlin, Heidelberg: Springer-Verlag.

Graham, B. P., & Cutsuridis, V. (2009). Dynamical information processing in the CA1 microcircuit of the hippocampus. In *Computational modelling in behavioural neuroscience: Closing the gap between neurophysiology and behavior*. London: Psychology Press, Taylor and Francis Group.

Graham, B., & Willshaw, D. (1995). Improving recall from an associative memory. *Biological Cybernetics*, *72*, 337–346.

Graham, B., & Willshaw, D. (1997). Capacity and information efficiency of the associative net. *Network*, *8*, 35–54.

Hasselmo, M., Bodelon, C., & Wyble, B. (2002). A proposed function of the hippocampal theta rhythm: Separate phases of encoding and retrieval of prior learning. *Neural Computation*, *14*, 793–817.

Hasselmo, M. E., & Kapur, A. (2000). Modelling of large networks. In E. De Schutter (Ed.)., *Computational neuroscience: Realistic modelling for experimentalists* (pp. 289–315). CRC Press.

Hebb, D. O. (1949). *The organization of behavior*. New York: John Wiley.

Houser, C. R. (2007). Interneurons of the dentate gyrus: An overview of cell types, terminal fields and neurochemical identity. *Progress in Brain Research*, *163*, 217–232.

Hunter, R., Cobb, S., & Graham, B. P. (2008a). Improving recall in an associative neural network of spiking neurons. In *LNCS*: *Vol. 5286*. *Dynamic brain - from neural spikes to behaviors* (pp. 137–141). Berlin, Heidelberg: Springer.

Hunter, R., Cobb, S., & Graham, B. P. (2008b). Improving associative memory in a network of spiking neurons. In *LNCS*: *Vol. 5164. Artificial neural networks - ICANN 2008* (pp. 636–645). Berlin, Heidelberg: Springer.

Jinno, S., Klausberger, T., Marton, L. F., Dalezios, Y., et al. (2007). Neuronal diversity in GABAergic long-range projections from the hippocampus. *Journal of Neuroscience*, *27*(33), 8790–8804.

Karmarkar, U. R., & Buonomano, D. V. (2002). A model of spike-timing dependent plasticity: One or two coincidence detectors?. *Journal of Neuroscience*, *88*, 507–513.

Klausberger, T., & Somogyi, P. (2008). Neuronal diversity and temporal dynamics: The unity of hippocampal circuit operations. *Science*, *321*, 53–57.

Klausberger, T., Magill, P. J., Marton, L. F., David, J., Roberts, B., Cobden, P. M., et al. (2003). Brain-state- and cell-type-specific firing of hippocampal interneurons in vivo. *Nature*, *421*, 844–848.

Klausberger, T., Marton, L. F., Baude, A., Roberts, J. D., Magill, P. J., & Somogyi, P. (2004). Spike timing of dendrite-targeting bistratified cells during hippocampal network oscillations in vivo. *Nat Neuroscience*, *7*(1), 41–47.

Kohonen, T. (1978). *Associative memory*. Springer-Verlag.

Kunec, S., Hasselmo, M. E., & Kopell, N. (2005). Encoding and retrieval in the CA3 region of the hippocampus: A model of theta-phase separation. *Journal of Neurophysiology*, *94*(1), 70–82.

Leung, L. S., Roth, L., & Canning, K. J. (1995). Entorhinal inputs to hippocampal CA1 and dentate gyrus in the rat: A current-source-density study. *Journal of Neurophysiology*, *73*(6), 2392–2403.

Lisman, J. (2005). The theta/gamma discrete phase code occurring during the hippocampal phase precession may be a more general brain coding scheme. *Hippocampus*, *15*, 913–922.

Lisman, J., & Idiart, M. A. (1995). Storage of 7 ± 2 short-term memories in oscillatory subcycles. *Science*, *267*, 1512–1515.

Lisman, J., & Spruston, N. (2005). Postsynaptic depolarization requirements for LTP and LTD: A critique of spike timing-dependent plasticity. *Nature Neuroscience*, *8*(7), 839–841.

Markram, H., Lubke, J., Frotscher, M., & Sakmann, B. (1997). Regulation of synaptic efficacy by coincidence of postsynaptic APs and EPSPs. *Science*, *275*(5297), 213–215.

Marr, D. (1971). A simple theory of archicortex. *Philosophical Transactions of the Royal Society of London B Biological Science*, *262*(841), 23–81.

Marr, D. (1969). A theory of cerebellar cortex. *Journal of Physiology (London)*, *202*, 437–470.

Menschik, E. D., & Finkel, L. H. (1998). Neuromodulatory control of hippocampal function: Towards a model of Alzheimer's disease. *Artificial Intelligence in Medicine*, *13*, 99–121.

Molyneaux, B. J., & Hasselmo, M. E. (2002). $GABA_B$ presynaptic inhibition has an in vivo time constant sufficiently rapid to allow modulation at theta frequency. *Journal of Neurophysiology*, *87*, 1196–1205.

Morgan, R., Santhakumar, V., & Soltesz, I. (2007). Modelling the dentate gyrus. *Prog Brain Research*, *163*, 639–658.

Morrison, A., Diesmann, M., & Gerstner, W. (2008). Phenomenological models of synaptic plasticity based on spike timing. *Biological Cybernetics*, *98*, 459–478.

Nishiyama, M., Hong, K., Mikoshiba, K., Poo, M., & Kato, K. (2000). Calcium stores regulate the polarity and input specificity of synaptic modification. *Nature*, *408*, 584–589.

Palm, G. (1982). *Neural assemblies: An alternative approach to artificial intelligence*. Springer-Verlag.

Palm, G. (1980). On associative memories. *Biological Cybernetics*, *36*, 9–31.

Palm, G. (1991). Memory capacities of local rules for synaptic modification. *Concepts in Neuroscience*, *2*, 97–128.

Palm, G., & Sommer, F. (1996). Associative data storage and retrieval in neural networks. In E. Domany, J. van Hemmen, & K. Schulten (Eds.), *Models of neural networks*: *Vol. II* (pp. 79–118). New York: Springer-Verlag.

Rubin, J. E., Gerkin, R. C., Bi, G. Q., & Chow, C. C. (2005). Calcium time course as a signal for spike-timing-dependent plasticity. *Journal of Neurophysiology*, *93*(5), 2600–2613.

Shouval, H. Z., Bear, M. F., & Cooper, L. N. (2002). A unified model of NMDA receptor-dependent bidirectional synaptic plasticity. *Proceedings of the National Academy of Sciences of the USA*, *99*, 10831–10836.

Soleng, A. F., Raastad, M., & Andersen, P. (2003). Conduction latency along CA3 hippocampal axons from rat. *Hippocampus*, *13*, 953–961.

Sommer, F. T., & Wennekers, T. (2000). Modelling studies on the computational function of fast temporal structure in cortical circuit activity. *Journal of Physiology (Paris)*, *94*, 473–488.

Sommer, F. T., & Wennekers, T. (2001). Associative memory in networks of spiking neurons. *Neural Networks*, *14*, 825–834.

Somogyi, P., & Klausberger, T. (2005). Defined types of cortical interneurons structure space and spike timing in the hippocampus. *Journal of Physiology*, *562*(1), 9–26.

Steinbuch, K. (1961). Non-digital learning matrices as preceptors. *Kybernetik*, *1*, 117–124.

Treves, A., & Rolls, E. (1994). Computational analysis of the role of the hippocampus in memory. *Hippocampus*, *4*, 374–391.

Tsukada, M., Aihara, T., Kobayashi, Y., & Shimazaki, H. (2005). Spatial analysis of spike-timing-dependent LTP and LTD in the CA1 area of hippocampal slices using optical imaging. *Hippocampus*, *15*, 104–109.

Van Geit, W., de Schutter, E., & Archard, P. (2008). Automated neuron model optimization techniques: A review. *Biological Cybernetics*, *99*, 241–251.

Willshaw, D., Buneman, O., & Longuet-Higgins, H. (1969). Non-holographic associative memory. *Nature*, *222*, 960–962.

Wittenberg, G. M., & Wang, S. S. H. (2006). Malleability of spike-timing-dependent plasticity at the CA3–CA1 synapse. *Journal of Neuroscience*, *26*, 6610–6617.

Wood, E., Dunchenko, P., & Eichenbaum, H. (1999). The global record of memory in hippocampal neuronal activity. *Nature*, *397*(6720), 613–616.

Please cite this article in press as: Cutsuridis, V., & Wennekers, T. Hippocampus, microcircuits and associative memory. Neural Networks (2009), doi:10.1016/j.neunet.2009.07.009